JOURNAL OF MATERIALS SCIENCE 13 (1978) 21–26

The occurrence of stress-induced α′ martensite in an (α+γ) Fe-Cr-Ni alloy

K. WAKASA*, T. NAKAMURA
Department of Materials Science and Engineering, Tokyo Institute of Technology, O-okayama, Meguro-ku, Tokyo, Japan

The interaction of an applied stress with the displacive shear during the martensitic transformation determined the *K–S* variants which formed in three types of tensile specimens, with tensile directions of 0°, 45° and 90° to a rolling direction respectively. The 3–6, 4–5 and 1–3 variants in a 0°-specimen, 1–5 and 4–5 variants in a 45°-specimen and 4–4 and 3–6 variants in a 90°-specimen are chosen as *K–S* variants which have the maximum value of U/σ in respective tensile directions. These variants are related to the occurrence of α' martensite with particular orientations as $(1\,0\,0)_\alpha$, $(1\,1\,0)_\alpha$ and $(2\,1\,1)_\alpha$.

1. Introduction

α' martensite is induced by a tensile stress in metastable austenitic Fe–Cr–Ni steels [1–3], the rate of transformation during straining depending upon the crystallographic direction of the applied stress [1], and the transformation structure depending on the direction of the applied stress [2]. In order to observe the anisotropic characteristics of martensite transformation, a γ phase recrystallized material was used. The integrated intensity of the $(1\,0\,0)_\alpha$, $(1\,1\,0)_\alpha$ and $(2\,1\,1)_\alpha$ increases as the amount of tensile deformation increases in the specimen, with tensile directions of 0°, 45° and 90° to a rolling direction [3]. In the 0°- and 45°-specimens, it was found that the proportional change in the integrated intensity ratio (I/I^0) with increasing tensile deformation for the $(2\,1\,1)_\alpha$ was significantly larger than for the $(1\,0\,0)_\alpha$ and $(1\,1\,0)_\alpha$, but in the 90°-specimen the ratio changed little with deformation. It is thus necessary to estimate how these features are related to the crystallographic direction of the applied stress.

2. Experimental procedure

The composition of the two-phase $(\alpha+\gamma)$ Fe–Cr–Ni steel used was 23.19% Cr, 4.91% Ni, 0.025% C, 1.47% Mo, 0.53% Si, 0.51% Mn, 0.91% Al, 0.023% P and the balance Fe. 2.0 mm thick sheets with tensile directions of 0°, 45° and 90° to a rolling direction were cut into tensile specimens with gauge sections of 6.0 mm × 18.0 mm. The specimens, that is, 0°-, 45°- and 90°-specimens, were annealed for 1 h at 1000° C to produce a mean grain size of 8.0 μm and 52% γ phase. The resultant recrystallization textures in α and γ phase had $(0\,0\,1)_\alpha[1\,1\,0]_\alpha$, and $(1\,1\,0)_\gamma[\bar{3}\,3\,2]_\gamma$ and $(2\,2\,5)_\gamma[\bar{2}\,\bar{3}\,2]_\gamma$ components, respectively [3].

Tensile deformations were carried out in the temperature range of −196° C to −50° C, using an Instron type testing machine operated at a crosshead speed of 0.5 mm min.$^{-1}$ The X-ray diffraction patterns of α and γ phase were obtained with Co$K\alpha$ radiation to examine the effect of the amount of deformation on the integrated intensity.

3. Results and discussion

3.1. The variation of the integrated intensity ratio in the α and γ phase

As the α' martensite is induced within γ phase of the two-phase alloy by a tensile stress, it is expected that the integrated intensities in diffracted-planes of α phase will vary as the amount of deformation increased, because the stress-induced α' martensite has the b c c structure [1–3]. In order to examine

*Present address: Institute for Medical and Dental Engineering, Tokyo Medical and Dental University, 2-3-10, Surugadi, Kanda, Chiyoda-ku, Tokyo, Japan.

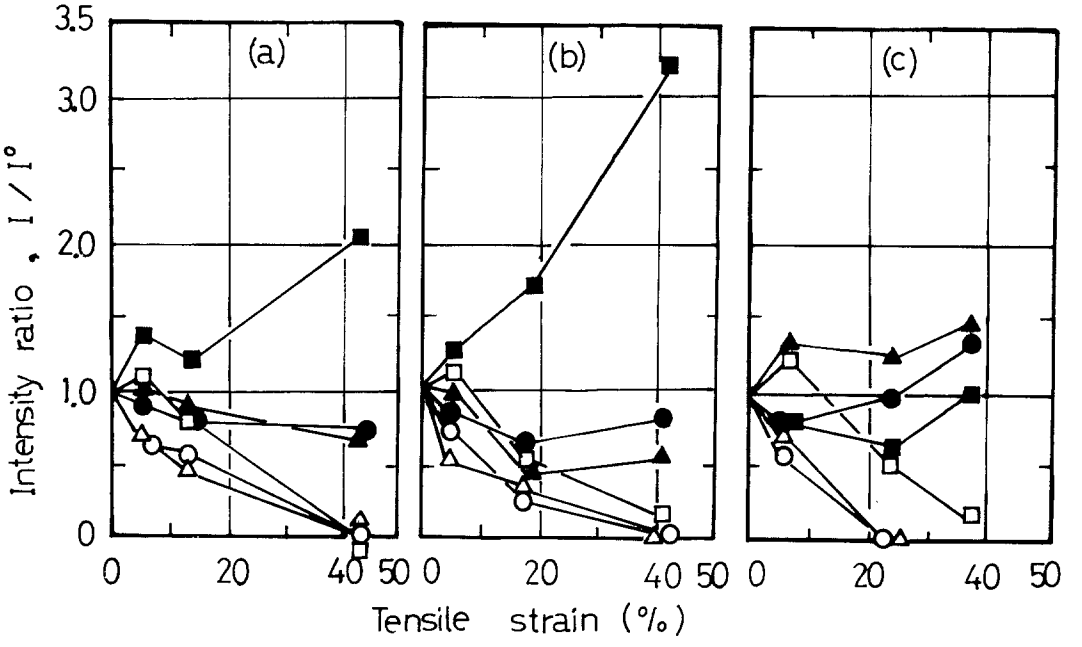

Figure 1 (a), (b) and (c). The variation of integrated intensity ratio (I/I^0) with tensile strain at −150° C in tensile specimens having tensile directions of 0°, 45° and 90° to a rolling direction: ■ $(2\,1\,1)_\alpha$, ▲ $(2\,0\,0)_\alpha$, ● $(1\,1\,0)_\alpha$, □ $(2\,0\,0)_\gamma$, △ $(2\,0\,0)_\gamma$, ○ $(1\,1\,1)_\gamma$.

how the integrated intensity in the specimens deformed to various tensile strains, I, increases or decreases with respect to the integrated intensity of the annealed specimen, I^0, at the diffracted-planes of α and γ phase, the integrated intensity ratio of I/I^0 was obtained. Consider, for example, the results obtained at −150° C which are shown in Figs. 1a, b and c. The intensity ratio in $(1\,1\,1)_\gamma$, $(2\,0\,0)_\gamma$ and $(2\,2\,0)_\gamma$ decreased with increasing amounts of deformation and reached a zero value because the γ phase had transformed to α' martensite during strain. The amount of α' martensite increased as the amount of deformation increased and test temperature decreased. This amount, for example, was 52% (0°-specimen), 52% (45°-specimen) and 52% (90°-specimen); 41% (0°), 41% (45°) and 35% (90°); 46% (0°), 42% (45°) and 38% (90°); and 33% (0°), 28% (45°) and 12% (90°) in fractured specimens at −196, −150, −102 and −50° C, respectively. In the specimens in which α' martensites were found, the ϵ martensite also occurred. The amount of ϵ martensite, however, did not increase with increasing deformation, and the largest recorded value was approximately 1.0% at any test temperature of −196, −150 and −102° C. The ϵ martensite which formed at −196, −150 and −102° C was first detected at tensile strains below 1.0%, 1.0% and 5.0%, respectively. There was no evidence of ϵ martensite at any strain at −50° C.

It is noted that the intensity ratio of the $(2\,1\,1)_\alpha$ in the 0°- and 45°-specimens increased to >2.0 and >3.0 at fracture strain, respectively. In the case of the 90°-specimen, the ratio of the $(2\,1\,1)_\alpha$ was approximately 1.0, and the ratios of the $(2\,0\,0)_\alpha$ and $(1\,1\,0)_\alpha$ were nearly 1.4 at fracture strain. These results obtained by X-ray measurement suggest the occurrence of α' martensite having orientations as $(2\,1\,1)_\alpha$, $(1\,1\,0)_\alpha$ and $(1\,0\,0)_\alpha$ parallel to the specimen surface. Similar results to the above were obtained when the 0°-, 45°- and 90°-specimens were deformed to various amounts of tensile strain of 1.0 to 67.0% at −196, −102 and −50° C. These results suggest that particular α' variants of lath martensite are being formed according to the crystallography of the applied stress and the specimen.

3.2. The interaction of an applied stress with the displacive shear during the martensite transformation

In order to estimate the effect of an applied stress on the formation of a particular α' variant, the following equation given by Machlin and Weinig [5] and Patel and Cohen [6] was used:

$$U/\sigma = \gamma_0 \cos\theta \cos\lambda + \epsilon_0 \cos^2\theta \qquad (1)$$

where U/σ = interaction of an applied stress with the displacive shear, θ = angle between the habit plane normal and the direction of tensile axis, and λ = angle between the shear direction and the direction of tensile axis. The values of γ_0 and ϵ_0 are equivalent to the components of the shear strain and the tensile strain in the direction of the particular transformation. In the present study, the $\{1\,1\,1\}_\gamma\ \langle 1\,1\,2\rangle_\gamma$ shear system [7] and the $\{1\,0\,1\}_\gamma\ \langle 1\,0\,1\rangle_\gamma$ shear system [8] were used, as these have been found to operate during the martensite transformation. The values of γ_0 and ϵ_0 are 0.192 and 0.089 for the $\{1\,1\,1\}_\gamma\ \langle 1\,1\,2\rangle_\gamma$ shear system, as calculated by Kelly [7], and the values of γ_0 and ϵ_0 are 0.224 and 0.026, respectively. The orientation relationships between the γ phase and the α' martensite were the Kurdjumov–Sachs relationships, reported by the present authors [9]. As there are 24 Kurdjumov–Sachs variants in the present Fe–Cr–Ni steel, it is necessary to obtain the values of U/σ for each of the variants in the relevant directions of the tensile axis [2, 10]. In order to calculate these values, the $(2\,0\,0)_\gamma$-pole figure was determined from X-ray measurements and is shown in Fig. 2. Two components of a recrystallization texture in the γ phase were identified and indexed as $(1\,1\,0)_\gamma\ [\bar{3}\,3\,2]_\gamma$ and $(2\,2\,5)_\gamma\ [\bar{2}\,\bar{3}\,2]_\gamma$. Tensile directions were chosen for two components to produce directions of 0°, 45° and 90° to the rolling direction. Fig. 3 shows the directions of the tensile axis in the $(0\,0\,1)_\gamma$ standard stereographic projection. For the $(1\,1\,0)_\gamma\ [\bar{3}\,3\,2]_\gamma$ component, the

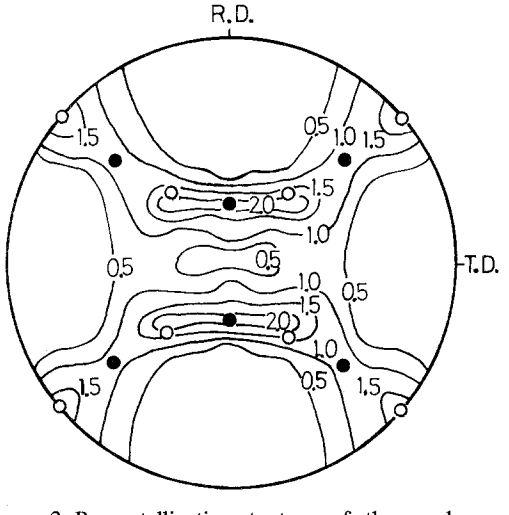

Figure 2 Recrystallization texture of the γ phase: ○ $(1\,1\,0)_\gamma\ [\bar{3}\,3\,2]_\gamma$, ● $(2\,2\,5)_\gamma\ [\bar{2}\,\bar{3}\,2]_\gamma$.

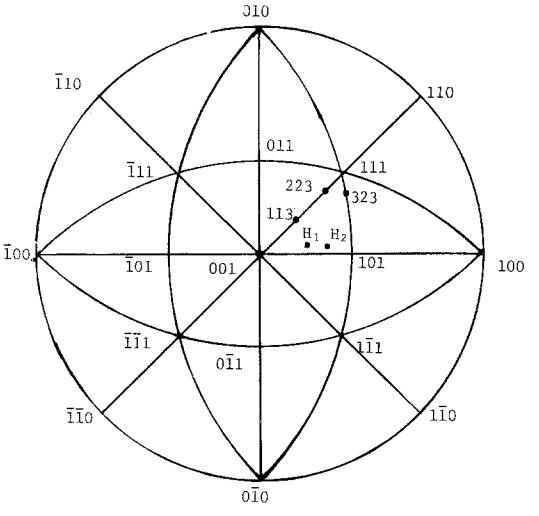

Figure 3 Relevant directions of the tensile axis to calculate the interaction of an applied stress with the displacive shear during the martensic transformation.

directions of the tensile axis for the tensile directions of 0°, 45° and 90° to the rolling direction were $[3\,2\,3]_\gamma$, $[0\,0\,1]_\gamma$ and $[1\,1\,3]_\gamma$, respectively, and for the $(2\,2\,5)_\gamma\ [\bar{2}\,\bar{3}\,2]_\gamma$ component, the directions which were equivalent to tensile directions of 0°, 45° and 90° to the rolling direction were $[2\,2\,3]_\gamma$, $[H_1]_\gamma$ and $[H_2]_\gamma$, respectively.

Table I shows the values of U/σ for the 24 variants of the six directions of the tensile axis in the $\{1\,1\,1\}_\gamma\ \langle 1\,1\,2\rangle_\gamma$ shear system. In this shear system, the habit plane and the direction of the transformation were $\{1\,1\,2\}_\gamma$ and $\langle 1\,1\,0\rangle_\gamma$, respectively. Therefore, only one value of U/σ is given for each variant. Table II shows the values of U/σ for the $\{1\,0\,1\}_\gamma\ \langle 1\,0\,1\rangle_\gamma$ shear system. In this case, two values of U/σ are obtained for each variant, because there are two sets of habit plane and direction of transformation. These sets of habit plane and direction of transformation were determined as $(0.602399, -0.777423, 0.180912)_\gamma$ and $[-0.154368, -0.159259, -0.046361]_\gamma$; $(0.180912, 0.777424, 0.602398)_\gamma$ and $[-0.04636, 0.159295, -0.154368]_\gamma$, using the Bowles–Mackenzie method [11].

3.3. The occurrence of stress-induced α' martensite

It is expected from Figs. 1a, b and c that a particular α' variant occurs during the martensitic transformation. In order to clarify this, the values of U/σ were calculated from the Equation 1, as shown in Tables I and II. These values had either

TABLE I Values of U/σ for the martensite transformation induced by a tensile stress in the $\{1\,1\,1\}_\gamma\langle 1\,1\,2\rangle_\gamma$ shear system

K–S relation		Variant notation	Values of U/σ					
Plane $(\gamma)\parallel(\alpha')$	Direction $[\gamma]\parallel[\alpha']$		Direction of tensile axis					
			[3 2 3]	[0 0 1]	[1 1 3]	[2 2 3]	$[H_1]$	$[H_2]$
$(\bar{1}\,1\,\bar{1})\,(1\,1\,0)$	$[1\,0\,\bar{1}]$ $[\bar{1}\,1\,\bar{1}]$	1–1	0.0624	−0.0406	−0.0115	0.0426	−0.0060	0.0175
	$[0\,\bar{1}\,1]$ $[\bar{1}\,1\,1]$	−2	0.0779	−0.0406	0.0000	0.0214	0.0000	0.0243
	$[\bar{1}\,\bar{1}\,0]$ $[\bar{1}\,1\,\bar{1}]$	−3	0.0779	0.0593	0.1106	0.1115	0.0675	0.0673
	$[\bar{1}\,0\,1]$ $[\bar{1}\,1\,1]$	−4	0.0674	0.0703	0.1103	0.1019	−0.0060	0.0175
	$[0\,1\,1]$ $[\bar{1}\,1\,\bar{1}]$	−5	−0.0455	0.0703	0.0000	−0.0424	0.0000	−0.0190
	$[1\,1\,0]$ $[\bar{1}\,1\,1]$	−6	−0.0455	0.0593	−0.0115	−0.0467	−0.0060	−0.0228
$(1\,1\,1)\,(1\,1\,0)$	$[\bar{1}\,0\,1]$ $[\bar{1}\,1\,\bar{1}]$	2–1	−0.0024	−0.0406	−0.0146	−0.0025	−0.0099	0.0072
	$[0\,\bar{1}\,1]$ $[\bar{1}\,1\,1]$	−2	0.0032	−0.0406	−0.0146	−0.0025	0.0000	0.0243
	$[1\,\bar{1}\,0]$ $[\bar{1}\,1\,\bar{1}]$	−3	0.0032	0.0593	0.0216	0.0035	0.0581	0.0397
	$[1\,0\,\bar{1}]$ $[\bar{1}\,1\,1]$	−4	−0.0024	0.0703	0.0250	0.0100	−0.0099	0.0072
	$[0\,1\,\bar{1}]$ $[\bar{1}\,1\,\bar{1}]$	−5	0.0036	0.0703	0.0250	0.0100	0.0000	−0.0145
	$[\bar{1}\,1\,0]$ $[\bar{1}\,1\,1]$	−6	0.0036	0.0593	0.0216	0.0035	0.0035	−0.0252
$(1\,\bar{1}\,\bar{1})\,(1\,1\,0)$	$[\bar{1}\,0\,\bar{1}]$ $[\bar{1}\,1\,\bar{1}]$	3–1	0.0717	−0.0406	0.0000	0.0214	−0.0219	0.0000
	$[0\,1\,\bar{1}]$ $[\bar{1}\,1\,1]$	−2	0.0547	−0.0406	−0.0115	0.0426	−0.0327	−0.0196
	$[1\,1\,0]$ $[\bar{1}\,1\,\bar{1}]$	−3	−0.0554	0.0593	−0.0115	−0.0467	0.0146	−0.0122
	$[1\,0\,1]$ $[\bar{1}\,1\,1]$	−4	−0.0499	0.0703	0.0000	−0.0424	0.0249	0.0000
	$[0\,\bar{1}\,1]$ $[\bar{1}\,1\,\bar{1}]$	−5	0.1104	0.0703	0.1103	0.1019	0.1321	0.1477
	$[\bar{1}\,\bar{1}\,0]$ $[\bar{1}\,1\,1]$	−6	0.1234	0.0593	0.1106	0.1115	0.1255	0.1499
$(\bar{1}\,\bar{1}\,1)\,(1\,1\,0)$	$[1\,0\,1]$ $[\bar{1}\,1\,\bar{1}]$	4–1	−0.0499	−0.0406	−0.0591	−0.0564	−0.0427	−0.0301
	$[0\,1\,1]$ $[\bar{1}\,1\,1]$	−2	−0.0554	−0.0406	−0.0591	−0.0564	−0.0495	−0.0363
	$[\bar{1}\,1\,0]$ $[\bar{1}\,1\,\bar{1}]$	−3	0.0547	0.0593	0.0864	0.0873	0.0349	0.0174
	$[\bar{1}\,0\,\bar{1}]$ $[\bar{1}\,1\,1]$	−4	0.0717	0.0703	0.1109	0.1046	0.0562	0.0355
	$[0\,\bar{1}\,\bar{1}]$ $[\bar{1}\,1\,\bar{1}]$	−5	0.1234	0.0703	0.1109	0.1046	0.1324	0.1497
	$[1\,\bar{1}\,0]$ $[\bar{1}\,1\,1]$	−6	0.1104	0.0593	0.0864	0.0873	0.1222	0.1417

plus or minus signs. It is assumed that the variants having plus signs form during tensile testing and the variants having minus values form during compression deformation. Assuming that at the low temperatures employed only tensile variants are possible. Table III shows the variants having the largest value of U/σ for the respective directions of the tensile axis in the $\{1\,1\,1\}_\gamma\langle 1\,1\,2\rangle_\gamma$ and $\{1\,0\,1\}_\gamma\langle 1\,0\,1\rangle_\gamma$ shear system. (In the $\{1\,0\,1\}_\gamma\langle 1\,0\,1\rangle_\gamma$ shear system, a twin relationship exists between the variants without a parenthesis and the variants with parenthesis.) The results obtained in Fig. 1 may be summarized as follows:

(1) In 0°- and 45°-specimens, the integrated intensity ratio of the $(2\,1\,1)_\alpha$ increased remarkably with increasing amounts of deformation and was >2.0 at fracture strain. This means that α' martensites having an orientation of $(2\,1\,1)_\alpha$ parallel to the specimen surface occurs during straining.

(2) In the 90°-specimen, the integrated intensity ratio of the $(2\,1\,1)_\alpha$ was approximately 1.0 at a fracture strain, and the integrated intensities of the $(2\,0\,0)_\alpha$ and $(1\,1\,0)_\alpha$ were nearly 1.5. This means that α' martensites having the orientations of $(1\,0\,0)_\alpha$ and $(1\,1\,0)_\alpha$ occur parallel to the specimen surface during straining.

It has already been noted (Section 3.1) that these trends occurred at all testing temperatures. In order to test the proposed model, the variants which had the largest values for directions of the tensile axis as $[3\,2\,3]_\gamma$, $[0\,0\,1]_\gamma$ and $[1\,1\,3]_\gamma$ were plotted on a stereographic net centred on $(1\,1\,0)_\gamma$ $[\bar{3}\,3\,2]_\gamma$, and the variants in $[2\,2\,3]_\gamma$, $[H_1]_\gamma$ and $[H_2]_\gamma$ were also plotted on the stereographic net centred $(2\,2\,5)_\gamma$ $[\bar{2}\,\bar{3}\,2]_\gamma$. From these projections, it followed that the orientation of $(2\,1\,1)_\alpha$ is near the centre of the stereographic net for the 0°- and 45°-specimens and the orientations of $(1\,0\,0)_\alpha$ and $(1\,1\,0)_\alpha$ are near the centre of the stereographic net in case of the 90°-specimen. The variants which lead to the observed results are indicated with an asterisk (*) in Table III, namely, variants 3–6 and 4–5, 1–5, 4–4, 1–3, 4–5, and 3–6 occurred with respect to $[3\,2\,3]_\gamma$, $[0\,0\,1]_\gamma$, $[1\,1\,3]_\gamma$, $[2\,2\,3]_\gamma$, $[H_1]_\gamma$ and $[H_2]_\gamma$ in case of $\{1\,1\,1\}\gamma\langle 1\,1\,2\rangle_\gamma$ shear system. In case of $\{1\,0\,1\}_\gamma$

TABLE II Values of U/σ for the martensite transformation induced by a tensile stress in the $\{1\,0\,1\}_\gamma\langle 1\,0\,1\rangle_\gamma$ shear system

Variant notation	Values of U/σ											
	Direction of tensile axis											
	[3 2 3]		[0 0 1]		[1 1 3]		[2 2 3]		$[H_1]$		$[H_2]$	
1–1	−0.0303	−0.0303	−0.0908	−0.0090	−0.0714	−0.0155	−0.0293	−0.0097	−0.0951	−0.0435	−0.0856	−0.0601
–2	0.0170	0.0500	−0.0908	−0.0090	−0.0563	0.0137	−0.0061	0.0261	−0.0592	0.0073	−0.0208	0.0374
–3	0.0170	0.0500	0.1241	0.1241	0.0978	0.0990	0.0539	0.0606	0.0787	0.0993	0.0056	−0.0514
–4	−0.0303	−0.0303	−0.0090	−0.0908	−0.0155	−0.0714	−0.0097	−0.0293	−0.0435	−0.0951	−0.0601	−0.0856
–5	0.0500	0.0170	−0.0090	−0.0908	0.0137	−0.0563	0.0261	−0.0061	0.0073	−0.0592	0.0374	−0.0208
–6	0.0500	0.0170	0.1241	0.1241	0.0990	0.0978	0.0606	0.0539	0.0993	0.0787	−0.0514	0.0056
2–1	−0.0504	−0.0504	−0.0908	−0.0090	−0.0860	−0.0201	−0.0496	0.0149	−0.0972	−0.0453	−0.0893	−0.0630
–2	−0.0058	0.0077	−0.0908	−0.0090	−0.0860	−0.0201	−0.0496	0.0149	−0.0602	0.0073	−0.0299	0.0300
–3	−0.0058	0.0077	0.1241	0.1241	0.0803	0.0803	0.0232	0.0232	0.0795	0.0982	0.0390	0.0155
–4	−0.0504	−0.0504	−0.0090	−0.0908	−0.0201	−0.0860	0.0149	−0.0496	−0.0453	−0.0972	−0.0630	−0.0893
–5	0.0077	−0.0058	−0.0090	−0.0908	−0.0201	−0.0860	0.0149	−0.0496	0.0073	−0.0602	0.0300	−0.0299
–6	0.0077	−0.0058	0.1241	0.1241	0.0803	0.0803	0.0232	0.0232	0.0982	0.0795	0.0155	0.0390
3–1	0.0026	0.0092	−0.0908	−0.0090	−0.0563	0.0137	−0.0061	0.0261	−0.0529	−0.0002	−0.0357	−0.0091
–2	0.0000	0.0255	−0.0908	−0.0090	−0.0714	−0.0155	−0.0293	−0.0097	−0.0465	0.0166	−0.0096	0.0391
–3	0.0100	0.0450	0.1241	0.1241	0.0990	0.0978	0.0606	0.0539	0.0943	0.1033	0.0594	0.0811
–4	0.0092	0.0084	−0.0090	−0.0908	0.0137	−0.0563	0.0261	−0.0061	−0.0002	−0.0529	−0.0091	−0.0357
–5	0.0255	0.0000	−0.0090	−0.0908	−0.0155	−0.0714	−0.0097	−0.0293	0.0166	0.0943	0.0391	−0.0096
–6	0.0450	0.0100	0.1241	0.1241	0.0978	0.0990	0.0539	0.0606	0.1033	−0.0465	0.0811	0.0594
4–1	0.0092	0.0084	−0.0908	−0.0090	−0.0420	−0.0218	0.0000	0.0218	−0.0546	−0.0019	−0.0358	−0.0098
–2	0.0100	0.0959	−0.0908	−0.0090	−0.0420	−0.0218	0.0000	0.0218	−0.0407	0.0166	0.0000	−0.0353
–3	0.0000	0.0255	0.1241	0.1241	0.0959	0.0959	0.0370	0.0370	0.0929	0.1035	0.0572	0.0829
–4	0.0084	0.0092	−0.0090	−0.0908	0.0137	−0.0420	0.0218	0.0000	−0.0019	−0.0546	−0.0098	−0.0358
–5	0.0450	0.0100	−0.0090	−0.0908	0.0137	−0.0420	0.0218	0.0000	0.0166	−0.0407	−0.0353	0.0000
–6	0.0255	0.0000	0.1241	0.1241	0.0450	0.0959	0.0370	0.0370	0.1035	0.0929	0.0829	0.0572

TABLE III K–S variants having the largest value of U/σ in two shear systems (A twin relationship was observed between the variant without a parenthesis and the variant with a parenthesis.)

Shear system $\{\gamma\}\langle 1\,1\,2\rangle$	Direction of tensile axis					
	[3 2 3]	[0 0 1]	[1 1 3]	[2 2 3]	$[H_1]$	$[H_2]$
$\{1\,1\,1\}\langle 1\,1\,2\rangle$	3–6* 4–5*	1–4, 1–5* 2–4, 2–5 3–4, 3–5 4–4, 4–5	4–4* 4–5	1–3* 3–6	3–5 4–5*	3–6* 4–5
$\{1\,0\,1\}\langle 1\,0\,1\rangle$	1–5 (1–2) 1–6 (1–3)*	1–3 (1–6)* 2–3 (2–6) 3–3 (3–6)* 4–3 (4–6)	3–3 (3–6) 1–6 (1–3)	1–6 (1–3)* 3–3 (3–6)*	3–6 (3–3) 4–6 (4–3)	4–6 (4–3) 3–6 (3–3)

*K–S variants which are in good agreement with the results obtained by X-ray analysis.

$\langle 1\,0\,1\rangle_\gamma$ shear system, 1–6(1–3), 1–3(1–6) and 3–3(3–6), 1–6(1–3) and 3–3(3–6), and 4–6 (4–3) occurred with respect to $[3\,2\,3]_\gamma$, $[0\,0\,1]_\gamma$, $[2\,2\,3]_\gamma$ and $[H_1]_\gamma$. In this case, there were no variants which satisfied the $[1\,1\,3]_\gamma$ and $[H_2]_\gamma$ tensile axes. It is therefore suggested that the $\{1\,1\,1\}_\gamma\ \langle 1\,1\,2\rangle_\gamma$ shear system is the dominant system in the present Fe–Cr–Ni alloy.

4. Conclusions

The values of U/σ for the 24 K–S variants for relevant directions of the tensile axis have been calculated from the equations which represented the interaction of an applied stress with the displacive shear during the martensitic transformation, in order to examine the crystallographic relationship during the formation of stress-induced α' martensite. The main results obtained were as follows:

(1) In 0°- and 45°-specimens, the integrated intensity ratio in the $(2\,1\,1)_\alpha$ was >2.0 at fracture strain in the temperature range -196 to -50° C, and the ratios in the $(2\,0\,0)_\alpha$ and the $(1\,1\,0)_\alpha$ were below 1.0. This means that α' martensite having a $(2\,1\,1)_\alpha$ plane is produced during the transformation.

(2) In a 90°-specimen deformed in the temperature range, the integrated intensity ratio in the $(2\,1\,1)_\alpha$ was close to 1.0 at fracture strain and the ratios in the $(2\,0\,0)_\alpha$ and $(1\,1\,0)_\alpha$ had the approximate values of 1.5. This means the formation of α' martensite with orientations of $(1\,0\,0)_\alpha$ and $(1\,1\,0)_\alpha$ parallel to the specimen surface dominates in this transformation.

(3) In the $\{1\,1\,1\}_\gamma\ \langle 1\,1\,2\rangle_\gamma$ shear system which dominates in the present Fe–Cr–Ni alloy, it is deduced that the 3–6 and 4–5 variants in $[3\,2\,3]_\gamma$ and 1–3 variant in $[2\,2\,3]_\gamma$, 1–5 variant in $[0\,0\,1]_\gamma$ and 4–5 variant in $[H_1]_\gamma$, and 4–4 variant in $[1\,1\,3]_\gamma$ and 3–6 variant in $[H_2]_\gamma$ occur in the 0°-, 45°- and 90°- specimens, respectively.

Acknowledgement

The authors are grateful to Mr Masanobu Kato who taught us about the crystallography of the martensite transformation.

References

1. R. LAGNEBORG, *Acta Met.* **12** (1964) 823.
2. D. GOODCHILD, W. T. ROBERTS and D. V. WILSON, *ibid* **18** (1970) 1137.
3. T. NAKAMURA and K. WAKASA, *Scripta Met.* 9 (1975) 959.
4. K. WAKASA and T. NAKAMURA, *ibid* **10** (1976) 129.
5. E. S. MACHLIN and S. WEINIG, *Acta Met.* **1** (1953) 480.
6. J. R. PATEL and M. COHEN, *ibid* **1** (1953) 531.
7. P. M. KELLY, *ibid* **13** (1965) 635.
8. Z. NISHIYAMA, "Elementary Martensite Transformation" (Maruzen Press, Japan, 1971) p. 245.
9. K. WAKASA and T. NAKAMURA, *J. Mater. Sci.* (to be published).
10. M. KATO and T. MORI, *Acta Met.* **24** (1976) 853.
11. J. S. BOWLES and J. K. MACKENZIE, *ibid* **2** (1954) 129.

Received 20 December 1976 and accepted 6 May 1977.